Applied Space-borne Remote Sensing to Identify Mass Movements and the Exemplary Modelling of Potentially Catastrophic Failures in the Bhagirathi Area, India

GWENDOLYN DASSER[1,2], JESSICA MUNCH[1,2], YVES BÜHLER[1,2], PERRY BARTELT[1,2] & ANDREA MANCONI[1,2]

Abstract: Extreme rainfall intensities, degrading permafrost and glacier melt in combination with ongoing construction of hydropower plants and settlement growth are leading to an ever-increasing amount of mass movements in alpine terrain. Geologically young mountain ranges such as the Indian Himalaya are experiencing severe consequences due to the combination of climatic changes and anthropogenic expansion, leading to higher risk for human lives and infrastructures. We present an approach to generate hazard indication maps of mass movements in high alpine areas using a combination of remote sensing and numerical simulations. We use satellite radar interferometry from Sentinel-1 and geomorphological feature classification based on optical satellite data. We show two exemplary case studies and model one of these to assess its hazard potential using the newly developed RAMMS::ROCKICE module.

1 Introduction

Systematic mapping, monitoring, and modelling of slope instabilities are essential tools for an effective hazard assessment, risk management and disaster response. Extreme topographic reliefs such as the Indian Himalayas are especially affected by current climatic changes such as weather extremes, glacier retreat or permafrost thawing (DAI et al., 2023). More and more large and potentially catastrophic mass movements are observed. Especially in the state of Uttarakhand, India, past events such as the rock and ice avalanche in Chamoli in 2021 (SHUGAR et al. 2021; VERMA et al. 2021; PANDLEY et al. 2022), have led to an increasing demand to identify and forecast potential geohazard scenarios. Several hydropower projects as well as new roads are currently under construction or in the planning phase in this area, increasing the risk to infrastructure and human lives (DEVARA et al. 2021), while also leading to further slope instabilities in the area (SATI et al. 2020).

Accurate measurements may allow detecting changes and/or precursors of such potentially catastrophic evolutions of mass movements. The Himalayas are a remote and challenging terrain, thereby strongly restricting the possibilities for in-situ measurements and especially systematic monitoring (DINI et al. 2019). Space-borne imagery allows a cost-effective possibility to provide regular information on such areas (STROZZI et al. 2004), also allowing to cover entire states, thereby complementing local measurements and observations (LIU et al. 2022).

[1] WSL Institute for Snow and Avalanche Research SLF, Alpine Remote Sensing, Flüelastrasse 111, CH-7260 Davos Dorf, Switzerland, E-Mail: [gwendolyn.dasser, andrea.manconi, yves.buehler, jessica.munch, perry.bartelt]@slf.ch

[2] Climate Change, Extremes and Natural Hazards in Alpine Regions Research Center CERC, Flüelastrasse 111, CH-7260 Davos Dorf, Switzerland

Mass movements such as landslides can be detected and classified at an early stage using a combination of interferometric data and optical imagery (JONES et al. 2021). Ground displacements can be measured at sub-centimetre scale using differential interferometric synthetic aperture radar (DInSAR; PASQUALI et al. 2014), thereby also allowing a detection of movements that might not yet be visible in the field (ZHOU et al. 2022). Such small-scale slope displacements may evolve over time and in some cases precede ultimate failures (MANCONI 2021). Optical remote sensing enables to retrace origin of movement to corresponding geomorphological processes. During cloud-free conditions, the usage of optical sensors also allows to cover areas that might be invisible to radar due to strong geometric effects in alpine areas. Hence, exploiting the combination allows to identify a higher amount and more diverse potential geohazards.

Current research of hazards in the state of Uttarakhand has been focused on post-event analysis. The rock and ice avalanche in Chamoli has been thoroughly examined by making use of satellite imagery, seismic records as well as eyewitness videos and numerical models (SHUGAR et al. 2021). Further research was conducted on the effect of vegetation loss to flash flood in the same case scenario (VERMA et al. 2021). Extensive hazard assessment using DInSAR is currently conducted over the area of Josimath, Uttarakhand, for diverse signs of ongoing ground movement have been found within the village (see DISCUSS TERRADUE 2023).

In this work, we present a workflow for large scale hazard analysis based on space-borne remote sensing for high alpine terrain of the Indian Himalaya. We provide a first attempt on systematic and spatially continuous assessment of unstable areas for the Bhagirathi valley using DInSAR. Using optical images, data gaps in radar-based images can be covered, and the identified mass movements specifically analysed to detect signs of activity and classify the geomorphological features. A cost-effective approach to further detect potential hanging glacier failures as seen in the event of Chamoli 2021 is also proposed. Two areas where catastrophic events may possibly develop in the future are then discussed in detail, and for one case the hazard potential is modelled using the Rock-Ice module of the RApid Mass Movement Simulation (RAMMS) tool.

2 Methods

2.1 Research Site

The Bhagirathi valley, located in the state of Uttarakhand in northern India, is of particular interest due to the amount of infrastructure and potentially exposed population in case of catastrophic events. The valley contains multiple smaller clusters of infrastructure such as the settlements of Bagori, Harshil and Naga, which are situated on the sedimented areas in river deltas and several hydropower projects in different state of planning and construction. The area experiences heavy rainfall during the Indian Summer Monsoon (BARNAND et al. 2004). Geomorphological analysis of the Bhagirathi catchment indicates periglacial processes present above 2000 m, while it being the driving factor above 4000 m elevation (SATI et al. 2020). The fluvial erosion, the location in periglacial zone and heavy and focussed rainfall lead to the valley being especially prone to mass movement activity (BARNARD et al. 2004) and hence being in the physiographic transition zone.

Fig. 1 indicates the geolocation of the research site featuring the extent of the area processed with DInSAR based on corresponding S1 tracks. Two locations are indicated, which are examples for identified hazards.
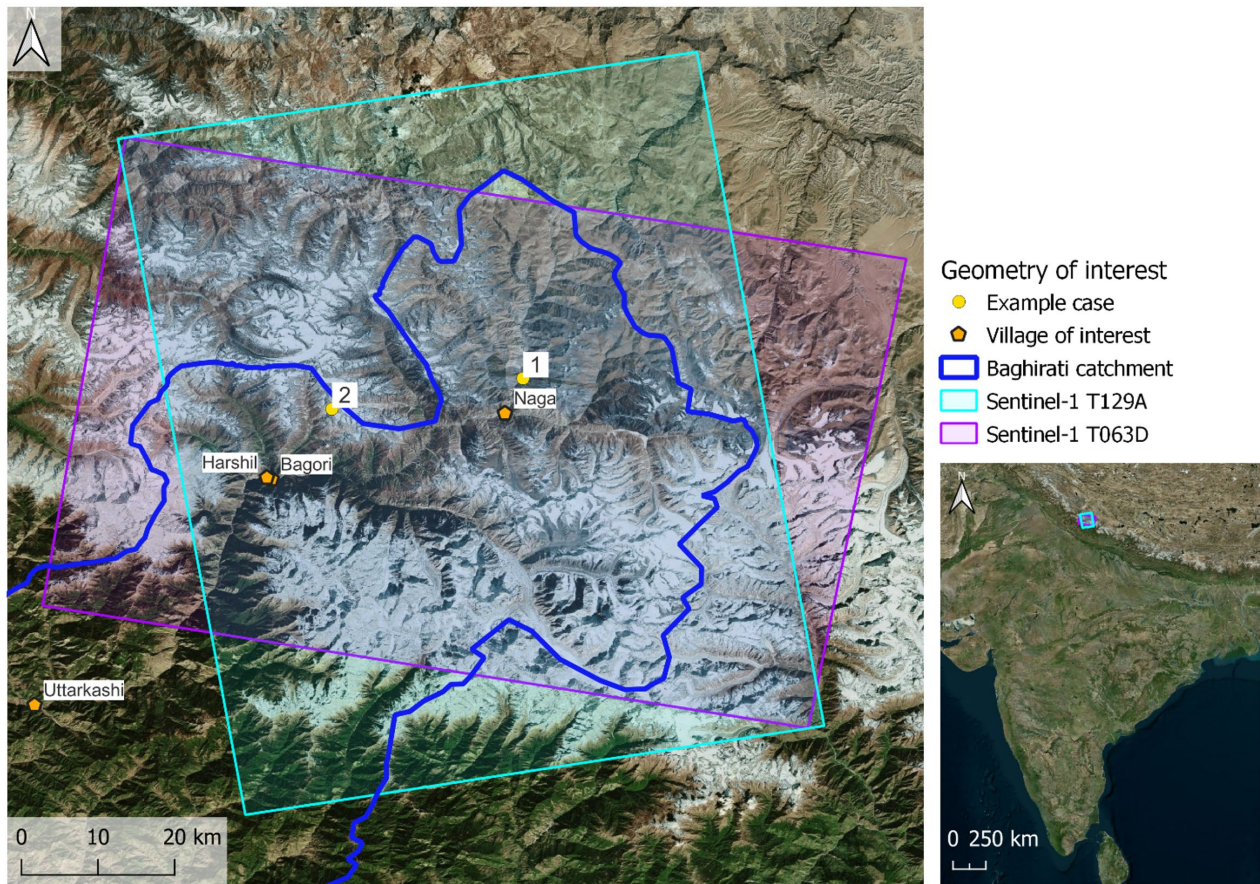
Fig. 1: Map featuring the locations of the two example cases and infrastructure of interest in the Bhagirathi valley, India. Indicated are used footprints from Sentinel-1 in ascending and descending node. Base map by BingAreal (Image acquisition date unknown).

2.2 Data and Preprocessing

Throughout this project we use a spectrum of remote sensing data and exploit combinations to detect, map and identify natural hazards. The combination of multiple data sources allows to capture various types of potentially catastrophic failures and enables to detect hazards which might be occluded in one stand-alone data analysis. We include information retrieved from Sentinel-1, Sentinel-2, PLANET, Bing Areal, Google Earth, digital elevation models (DEM), as well as a publicly available permafrost layer (GRUBER 2012) and glacier inventory (GLIMS CONSORTIUM 2005).

We process and analyse satellite radar datasets acquired from the ESA Sentinel-1 (S1) mission in the period 2018-2021 for the footprints indicated in Fig. 1. We selected one ascending (T129) and one descending (T063) track to gain information in two line-of-sight directions (LOS), thereby minimizing the number of shadowed areas. The SAR dataset is composed of 117 images in ascending and 103 images in descending orbit. We use standard DInSAR to first identify and then classify areas affected by potential instabilities. Interferograms were computed by selecting image-pairs based on perpendicular baseline below 3 m and temporal baseline of below 1 year. This resulted in a dataset featuring interferometric baselines between 12 to 300 days. From these, interferograms were manually discharged, where visual analysis indicated coherence within the Bhagirathi valley to not be feasible. Information on the interferograms is summarized in table 1.

We made use of a combination of base map analysis by Google Earth, Bing areal and PLANET data. We included PLANET data, even though the spatial resolution is coarser, to analyse deformation changes over specific timeframes. Selection of dates of PLANET acquision is indicated in table 1 and was done by searching for the most feasible trade-off between snow, cloud and areal coverage while covering at least all summer seasons.

Tab. 1: Temporal windows of S1 image-pairs per track and acquisition date of selected PLANET data

Track 129 ascending		Track 063 descending		PLANET
Primary image	Secondary image	Primary image	Secondary image	
30.08.2018	26.06.2019	22.01.2018	10.05.2018	22.01.2018
30.10.2020	09.07.2021	22.05.2018	21.07.2018	22.05.2018
23.11.2020	23.03.2021	16.07.2019	21.08.2019	04.08.2018
05.12.2020	17.12.2020	29.04.2020	04.06.2020	23.07.2019
05.12.2020	03.02.2021	26.10.2020	18.01.2021	07.09.2019
17.12.2020	03.02.2021	26.10.2020	05.07.2021	12.06.2020
23.03.2021	14.08.2021	18.01.2021	05.07.2021	19.10.2020
				27.02.2021
				01.07.2021

In the framework of this project, we used a publicly available glacier inventory (GLIMS CONSORTIUM 2005) to identify possible hanging glaciers by intersecting the dataset with a slope mask of above 25 degrees. This terrain slope was calculated from the 30 m Copernicus digital elevation model (DEM). To better identify features created through processes in connection to permafrost, the freely available global permafrost zonation indication map (GRUBER 2012) was consulted.

2.3 RAMMS::ROCKICE simulations

RAMMS::RockIce is a thermo-mechanical module from the RAMMS software (CHRISTEN et al., 2010, BARTELT et al., 2018) that is specifically designed to model gravitational flows made of rock/ice/water/snow or any combination of these. The module is based on the depth-averaged conservation of mass, momentum, and energy for all the phases involved in the flow and allows for interactions in between the phases, such as heat transfer between the different materials as the temperature of each material is computed separately during a simulation. This means that the ice can melt and turn into water, increasing the water content of the flow and potentially the runout distances (SCHNEIDER et al. 2011). The module also allows for ground material entrainment following (FRANK et al. 2015), which again can impact the distances travelled by the flow.

In this work, we are interested in different setups for gravitational movements, involving different kinds of materials. Firstly, we are investigating a deep seated landslide, and secondly an ice avalanche starting from a hanging glacier. The remote sensing methodology, the numerical modelling as well as the main results for one of these cases will be developped in part 3.3.

3 Identified geomorphological hazards and their modelling

3.1 Geohazard assessment in the greater Bhagirathi area

The examination of interferograms fringe patterns across diverse baselines, allows a detection and mapping of mass movements featuring different velocities. By analysing images acquired using ascending and descending tracks, movement in west-east and east-west, respectively, can be detected. By visual comparison of fringe patterns to optical imagery geomorphological features were identified. In this study, these features mainly included landslides, (rock) glaciers and fluvial sediment relocations. Large deep-seated landslides were often detectable across temporal baselines; however, the smaller temporal windows allowed to differentiate and detect also faster, secondary landslides.

Above-average mass movement activity in two side valleys neighbouring the Bhagirathi valley were identified, including two large instabilities with a velocity of more than 30 cm/year in descending LOS). Around twenty more areas show velocities of more than 15 cm/year in more than one interferogram. In the following, we selected two example cases based on the potential impact on infrastructure and corresponding hazard potential.

3.2 Example case 1: Deep seated landslide failure

We discuss here an example of a large, deep-seated landslide, which already resulted in visible displacement in optical imagery. At the bottom of the landslide, a river connects the moving area to the village of Naga, further downstream. The river course has been altered due to ground movement and a crest is visible (see Fig. 2). A road follows this river, also being built upon the landslide area. The road crosses the river twice via bridges on the way downstream to the city of Naga. DInSAR data indicates the landslide to be a complex moving system featuring different layers and velocities. According to the permafrost layer created in 2018, permafrost presence is possible but uncertain. With a global decrease in permafrost, the slope instability might therefore be caused or at least fostered by permafrost degradation processes. The interferograms indicate three different movement zones (see Fig. 4).

Fig. 2: Situation of landslide case study in relation to a bridge, the village of Naga on Bing Areal base maps (Image acquisition date unknown).

In the framework of this report, we analyse one scenario of a sudden release of a part of this landslide, beginning at the indicated visible crest (see Fig. 2). Depth of this moving ground mass has been estimated via the area of the landslide and the equation and variables provided in JONES (2021) to be around 20 m.

Tab. 2: Temporal windows of interferograms (primary image named first), the corresponding temporal baseline, the detected range of fringes and calculated surface velocity when upscaled to a year

Temporal window interferograms [dd.mm.yyyy – dd.mm.yyyy]	Temporal baseline [days]	Surface velocity away from LOS [cm/year]
22.01.2018 – 10.05.2018	108	2.4 to 4.7
22.05.2018 – 21.07.2018	60	8.5 to 11.3
16.07.2019 – 21.08.2019	36	14.2 to 28.4
29.04.2020 – 04.06.2020	36	14.2 to 28.4
26.10.2020 – 18.01.2021	92	5.6 to 11.1
26.10.2020 – 05.07.2021	252	4.1 to 8.1
18.01.2021 – 05.07.2021	168	6.1 to 12.2
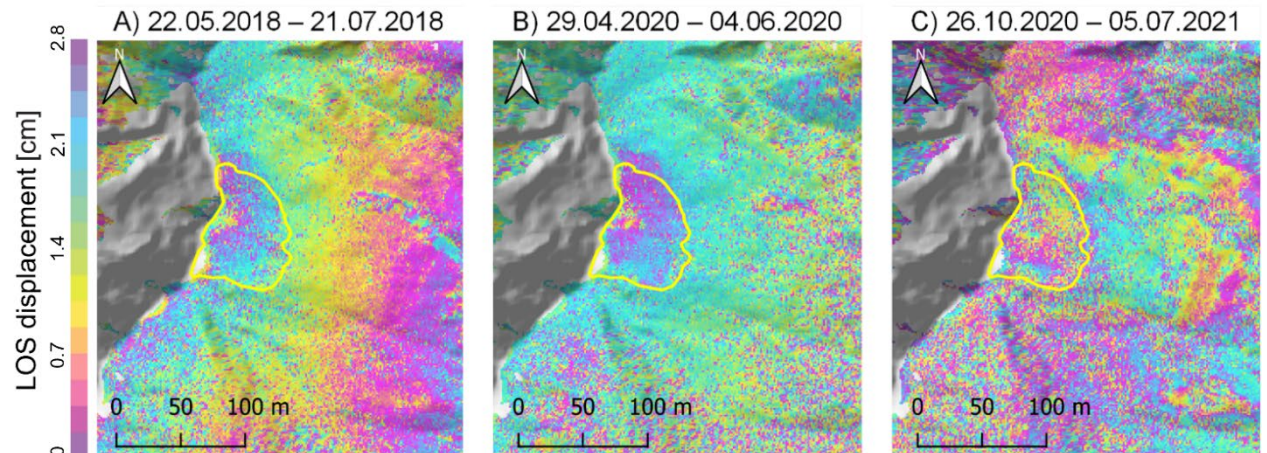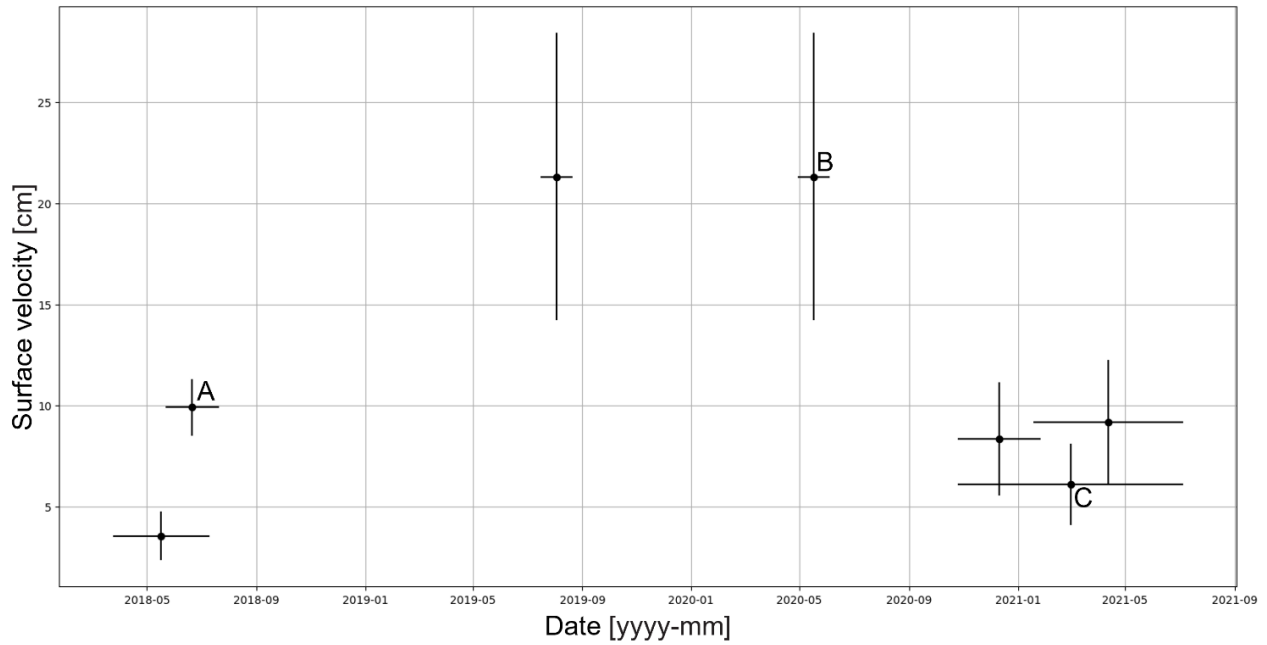
Fig. 3: Magnitude of estimated surface velocities of the slope deformation across interferograms featuring different time windows in descending orbit and three exemplary interferograms

The results of the interferometric analysis of images are summarized in Tab. 2 and illustrated in Fig. 3. Only interferograms in descending orbit were feasible for the detection of this movement

due to the orientation in relation to the LOS. Each interferogram indicates an occurring phase difference (see examples in Fig. 3).

The interferogram of May 2018 to July 2018 shown in Fig. 3.A) indicates movement, also visible is large-scale atmospheric phase delay, which is correlated with topography. Between April and July 2020 (Fig. 3.B) a secondary, faster landslide within the delineated, already moving area, is apparent. The phase difference between October 2020 and July 2021 (Fig. 3.C) indicates a further complexity of the moving mass, as a third, even larger area is also – however, more slowly – moving.

Derived surface velocities are constantly above background noise. Highest surface velocities are found in interferograms of smallest temporal baseline. This indicates sharp increase of surface displacements, which might be due to snowmelt in spring, or heavy rainfall during the monsoon season. Longer temporal windows average the movement over time, resulting in lower velocity values, as to be expected (see Fig. 3).

These findings show clear signs of surface deformation over time. Slopes characterised by such ongoing movements are instable and can be triggered in case of extreme rainfall intensity/duration or an earthquake, leading to a sudden release and a potentially catastrophic outcome. Together with the vicinity of the landslide to infrastructure such as the bridge indicated in Fig. 2 and the village of Naga further downstream, this landslide poses threat to human lives in such a case. Currently, we are in the modelling phase of potential scenarios and first results indicate a strong dependency of atmospheric precipitation on the landslides hazard potential.

3.3 Example case 2: Hanging glacier failure

The rock and ice avalanche of Chamoli has shown hanging glaciers to pose risk in case of sudden release (SHUGAR et al. 2021). However, glacier movement is near to impossible to detect on interferometric data, as the highly dynamic environment is changing too rapidly for phase analysis to be effective. We therefore used the global glacier inventory. Using an intersection between slope above 25 degrees and the glacier inventory, a hanging glacier library was created for the area of interest. This library was imported to Google Earth and the potential hazard for infrastructure manually assessed for each case. The glacier with the highest hazard potential was selected and further investigated. Based on optical images, the most likely failure scenario was delineated, following already visible crevasses in the glacier (see Fig. 4). Glacier depth of 50 m was estimated by averaging glacier front measurements at the possible failure location in Google Earth.

The release zone was defined as a block of pure ice, with a depth of 50 m and a total volume of ~250 000 m³. The release area was delineated between two sets of converging cracks in the glacier as found in optical imagery (see Fig. 4).

Two different scenarios of this hanging glacier release were modelled using RAMMS::ROCKICE. The two scenarios diverge only in the presence of atmospheric snow cover: We defined a snow-free and a snow-rich scenario for the track of the ice avalanche. In the latter, 7 m of snow cover depth was added to the model, starting at release zone with a reduction of 0.03 m per 100 m elevation decrease.
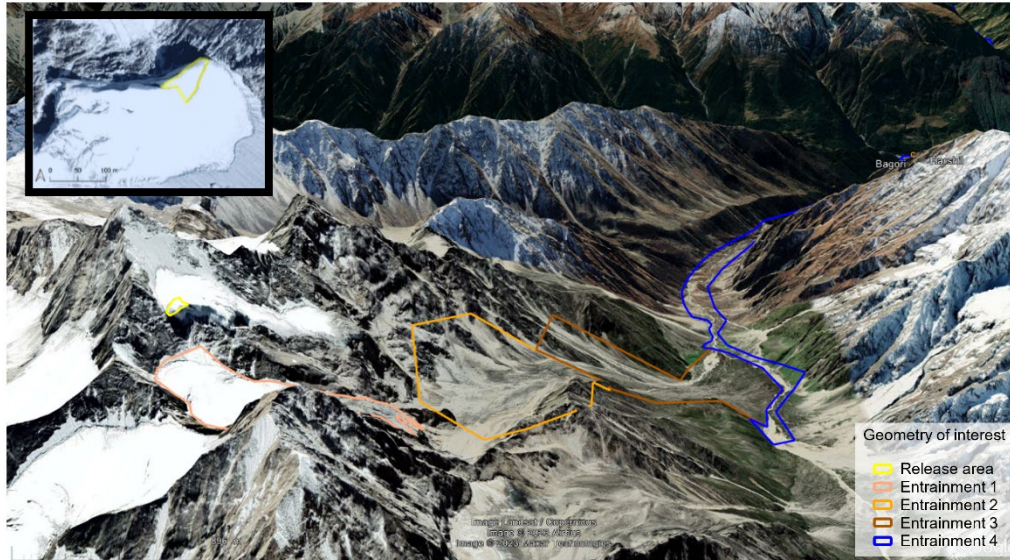
Fig. 4:   Situation of potential hanging glacier failure in relation to the villages of Bagori and Harshil and a top view on the delineated failure part (image from 18/8/2022, Google Earth). Indicated are the applied entrainment zones (parameters described in part 3.3)

The potential runout path in case of failure covers diverse terrains. These range from glacier over pre-glacial sediments and a sediment cone to the river-basin. To model this range of terrain types, we defined four different entrainment zones that are shown in Fig. 4 and the parameters selected are summarized in table 3. The release as well as each of the entrainment layers were set at a temperature of 0 °C in both scenarios. The simulations were ran for 3000 s or until the momentum of the flow was less than 3% of its initial value.

Table 3: Parameters set for each entrainment zone in both case scenarios in case of glacial collapse.

Entrain-ment [No.]	Material composition [rock%, ice%, water%]	Density [kg/m^{-3}]	Erosion rate [m/s^{-3}]	Potential erosion depth [m]	Critical shear stress [kPa]	Maximal erosion depth [m]
1	0, 95, 5	1000	0.013	0.100	1	10
2	60, 30, 10	2000	0.013	0.100	1	10
3	75, 15, 10	2400	0.05	0.1	0.5	10
4	80, 0, 20	2500	0.05	0.2	0.5	10

In the snow-free glacier collapse scenario (Fig. 5.A), areas affected by the released material is minimal. The short runout also results in a very limited effect of entrained material. In the snow-rich scenario however (Fig. 5.B), the snow cover results in more material present in the release at model initiation, but also in the entrainment zones. This leads to a longer runout due to more material being entrained and also a potential to produce a higher amount of meltwater as both snow and ice as susceptible to melt. High water content in mass movement increases the mobility of the materials and thus their potential for destruction at further distances (SCHNEIDER et al., 2011). This is due to water reducing the ground friction as reported in the case of Chamoli 2021 (SHUGAR et al. 2021). The resulting higher velocity and longer runout of the moving mass results in more mass being transported downstream. In this scenario, calamities and economic losses are to be expected.

The current snow-rich scenario setup and corresponding parameters used, indicates a complete destruction of the villages of Harshil and Bagori.
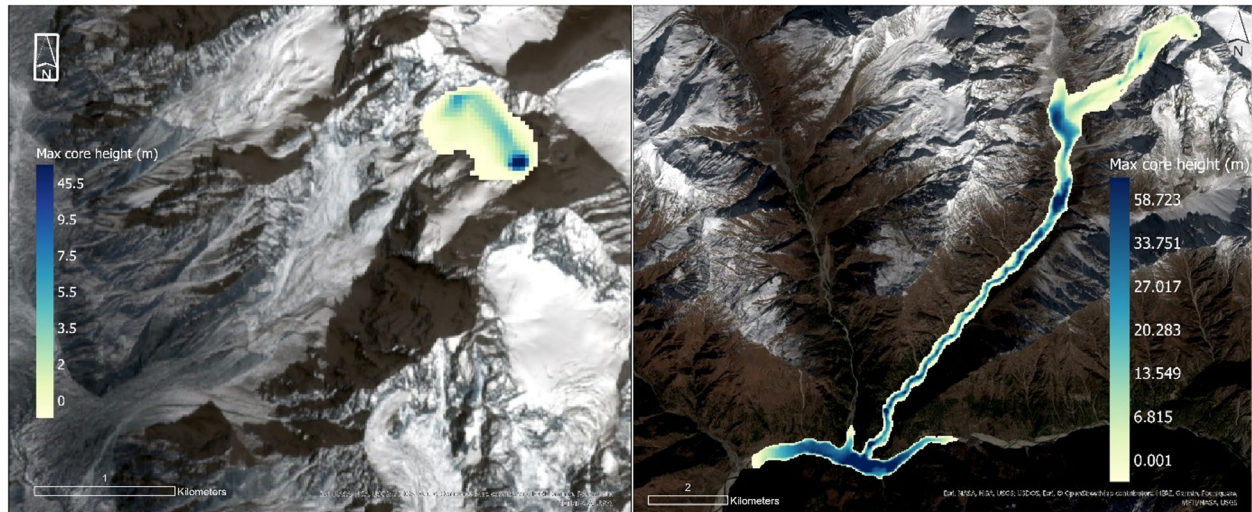
Fig. 5: RAMMS simulations of the ice avalanche for two scenarios. The maximal core height in meters is shown for the hanging glacier collapse for a snow-free (left, A) and snow-rich (right, B) scenario including entrainment. Background map is the Sentinel-2 RGB-image acquired on 11.04.2022.

3.4 Challenges

A visual analysis of the entire Bhagirathi valley as performed here is time consuming. Hitherto, no automatization process is in place to make such a hazard indication map generation more efficient. Currently we need to filter areas to efficiently map ground movement with highest impact potential. In the framework of this project, we focus on higher elevations zones, where glaciers and permafrost are key components in the landscape. The event at Chamoli has shown that ice can lead to an even more catastrophic result when melted by frictional heat (SHUGAR et al. 2021). We thus include in our geohazard assessment also processes of corresponding nature. The consultation of external datasets for e.g. glacier localisation might result in further uncertainties in the processing chain. For being a highly dynamic environment, archives based on historic data might not be up to date or datasets might feature data gaps we overlooked. This could result in missing out potentially failing geohazards. As a result, we do not capture all potentially hazardous events and are still limited in spatial coverage due to high processing and working costs.

High alpine terrain as the one present includes a range of challenges for remote sensing approaches. DInSAR images for example suffer from geometric effects such as shadowing, foreshortening and layover (MANCONI 2021). Atmospheric phase delay is further amplified in terrain featuring high topographic gradients (CIGNETTI et al. 2016), rendering the technique partly inapplicable in such areas. Vegetational activity and heavy rainfall events such as the Monsoon result in decorrelation of image pairs, further restricting the usage of phase information. Fast and complex ground movement can further lead to phase ambiguity. Geometric restrictions of spaceborne radar also makes it impossible to capture movement in unsuitable movement directions (COLESANTI & WASOWSKI 2006). DInSAR datasets therefore allow to detect some movement in alpine terrain, however it does not cover all hazard types or movement directions, nor does it provide gap free information (MANCONI 2021).

284

When performing the modelling, multiple assumptions had to be made, mostly regarding the composition of the entrainment layers. In this study, we estimated such parameters based on optical satellite image interpretation, as well as on experience gained from modelling other mass movements containing rock/ice/water/snow or a mixture of these, such as the post-event modelling of Chamoli. As water content in the flow has a major impact on the runout distances of the modelled flows, the results are highly dependent on the composition and physical properties of the release and entrainment zones; and are only valid within the framework of the assumptions that were made. The models were run for two scenarios, one featuring snow coverage and one free of snow. Further research should include also other effects of seasonality and weather extremes such as the Monsoon, as for heavy rainfall results in a higher water content in all influenced stages of entrainment, leading to larger runouts and changes in fluid dynamics. Larger amounts of water can further trigger potential (additional) landslides in the flow.

By highlighting the influence of the composition of the release zone and entrainment layers, we want to further insist on the importance of field observations and measurements. These are required to better understand geomorphological features present, the compounds and extents of possible entrainment zones included in the process and climatic and weather data.

4   Conclusions & Outlook

Using a combination of various remote sensing techniques, we provide a first assessment on potential hazards present in the Bhagirathi area. By exploiting high resolution optical imagery such as provided by PLANET and Google Earth, we classified ground deformation information mapped using DInSAR according to geomorphological processes. Our results indicate deep seated landslides moving up to 30 cm/year, accelerating rock glaciers as well as highly dynamic hanging glaciers to be potential geohazards present in the Bhagirathi area.

Based on two different case studies, we discussed challenges and opportunities of the different datasets and showed that for a complete hazard indication map a combination of datasets is invaluable. Using DInSAR technology in combination with optical image analysis, a complex landslide was detected, which features movement already over several years and with estimated velocities of up to 14-28 cm/year. Using a combination of glacier inventories, optical imagery, and slope information, we identified potential hazard through hanging glacier collapses.

With the usage of the new Rock-Ice avalanche module in RAMMS, we delineated the potential hazard in one case study. It indicated strong potential for calamities and destruction of downstream infrastructure especially in scenarios containing high amounts of snow and ice. This further highlights the effect of atmospheric precipitation on the hazard potential of such scenarios.

We pursue this project further by setting up a workflow for entire Uttarakhand and providing an overview on mass movement activity in the area with potential catastrophic consequences. This enables local researchers to focus on areas of potential hazards. Specific field work can then be conducted to minimize uncertainties in hazard modelling by increasing the understanding of the local environment. In the framework of planned workshops, we also transfer knowledge on the processing workflow to local researchers in India, allowing to create a dynamic mass movement inventory of the state of Uttarakhand.

5 Acknowledgment

6 Literature

BARTELT, P., CHRISTEN, M., BÜHLER, Y. & BUSER, O., 2018: Thermomechanical modelling of rock avalanches with debris, ice and snow entrainment. Numerical methods in geotechnical engineering IX, Porto, PT, 1047-1054.

BARNAND, P.L., OWEN, L.A. & FINKEL, R.C., 2004: Style and timing of glacial and paraglacial sedimentation in a monsoon-influenced high Himalayan environment, the upper Bhagirathi Valley, Garhwal Himalaya. Sedimentary Geology, **165**, 199-221.

CHRISTEN, M., KOWALSKI, J. & BARTELT, P., 2010. RAMMS: Numerical simulation of dense snow avalanches in three-dimensional terrain. Cold Regions Science and Technology, **63**, 1-14.

CIGNETTI, M., MANCONI, A., MANUNTA, M., GIORDAN, D., DE LUCA, C., ALLASIA, P. & ADRIZZIONE, F., 2016: Taking Advantage of the ESA G-POD Service to Study Ground Deformation Processes in High Mountain Areas: A Valle d'Aosta Case Study, Northern Italy. Remote Sensing, **8**(852).

COLESANTI, C. & WASOWSKI, J., 2006: Investigating landslides with space-borne Synthetic Aperture Radar (SAR) interferometry. Engineering Geology, **88**, 173-199.

DAI, C., LI, W., LU, H. & ZHANG, S., 2023: Landslide Hazard Assessment Method Considering the Deformation Factor: A Case Study of Zhouqu, Gansu Province, Northwest China. Remote Sensing, **15**(596).

DEVARA, M., TIWARI, A. & DWIVEDI, R., 2021: Landslide susceptibility mapping using MT-InSAR and AHP enabled GIS-based multi-criteria decision analysis. Geomatics, Natural Hazards and Risk, **12**(1), 675-693.

DINI, B., DAOUT, S., MANCONI, A. & LOEW, S., 2019: Classification of slope processes based on multitemporal DInSAR analyses in the Himalaya of NW Bhutan. Remote Sensing of Environment, **233**(111408).

DISCUSS TERRADUE, 2023: Results of advances InSAR services (Sentinel-1) indicate that the town of Joshimath (Northern India) is sliding. https://discuss.terradue.com/t/results-of-advanced-insar-services-sentinel-1-indicate-that-the-town-of-joshimath-northern-india-is-sliding/1149, last accessed on 30.1.2023.

FRANK, F., MCARDELL, B.W., HUGGEL, C. & VIELI, A., 2015: The importance of erosion for debris flow runout modelling from applications to the Swiss Alps. Natural Hazards Earth System Sciences Discussions, **3**, 2379-2417.

GLIMS CONSORTIUM, 2005: GLIMS Glacier Database. Version 1. Boulder Colorado, USA. NASA National Snow and Ice Data Center Distributed Active Archive Center. https://doi.org/10.7265/N5V98602.

GRUBER, S., 2012: Derivation and analysis of a high-resolution estimate of global permafrost zonation. The Cryosphere, **6**, 221-233. https://doi.org/10.5194/tc-6-221-2012.

JONES, N., MANCONI, A. & STROM, A., 2021: Active landslides in the Rogun Catchment, Tajikistan, and their river damming hazard potential. Landslides, **18**, 3599-3613.

LIU, Z., QIU, H., ZHU, Y., LIU, Y., YANG, D., MA, S., ZHANG, J., WANG, Y., WANG, L. & TANG, B., 2022: Efficient Identification and Monitoring of Landslides by Time-Series InSAR Combining Single- and Multi-Look Phases. Remote Sensing, **14**(1026).

MANCONI, A., 2021: How phase aliasing limits systematic space-borne DInSAR monitoring and failure forecast of alpine landslides. Engineering geology, **287**(106094).

PANDEY, V.K., KUMAR, R., SINGH, R., KUMAR, R., RAI, S.C., SINGH, R.P., TRIPATHI, A.K., SONI, V.K., ALI, S.N., TAMANG, D. & LATIEF, S.U., 2021: Catastrophic ice-debris flow in the Rishiganga River, Chamoli, Uttarakhand (India). Geomatics, Natural Hazards and Risk, **13**(1), 289-309.

PASQUALI, P., CANTONE, A., RICCARDI, P., DEFILIPPI, M., OGUSHI, F., GAGLIANO, S. & TAMURA, M., 2014: Mapping of Ground Deformations with Interferometric Stacking Techniques. Land Applications of Radar Remote Sensing, InTech.

SATI, S.P., SHARMA, S., SUNDRIYAL, Y.P., RAWAT, D. & RIYAL, M., 2020: Geo-environmental consequences of obstructing the Bhagirathi River, Uttarakhand Himalaya, India. Geomatics, Natural Hazards and Risk, **11**(1), 887-905.

SCHNEIDER, D. & HAEBERLI, W., 2011. On characteristics and flow dynamics of large rapid mass movements in glacial environments. Doctoral thesis, Department of Geography, University of Zurich.

SHUGAR, D.H., JACQUEMART, M., SHEAN, D., BHUSHAN, S., UPADHYAY, K., SATTAR, A., SCHWANGHART, W., MCBRIDE, S., VAN WYK DE VRIES, M., MERGILI, M., EMMER, A., DESCHAMPS-BERGER, C., MCDONNELL, M., BHAMBRI, R., ALLEN, S., BERTHIER, E., CARRIVICK, J.L., CLAGUE, J.J., DUKUKIN, M., DUNNING, S.A., FREY, H., GASCOIN, S., HARITASHYA, U.K., HUGGEL, C., KÄÄB, A., KARGEL, J.S., KAVANAUGH, J.L., LACROIX, P., PETLEY, D., RUPPER, S., AZAM, M.F., COOK, S.J., DIMRI, A.P., ERIKSSON, M., FARINOTTI, D., FIDDES, J., GNYAWALI, K.R., HARRISON, S., JHA, M., KOPPES, M., KUMAR, A., LEINSS, S., MAJEED, U., MAL, S., MUHURI, A., NOETZLI, J., PAUL, F., RASHID, I., SAIN, K., STEINER, J., UGALDE, F., WATSON, C.S. & WESTOBY, M.J., 2021: A massive rock and ice avalanche caused the 2021 disaster at Chamoli, Indian Himalaya. Science, **373**, 300-306.

STROZZI, T., KÄÄB, A. & FRAUENFELDER, R., 2004: Detecting and quantifying mountain permafrost creep from in situ inventory, space-borne radar interferometry and airborne digital photogrammetry. International Journal of Remote Sensing, **25**(15), 2919-2931.

VERMA, S., SHARMA, A., YADAVA, P., GUPTA, P., SINGH, J. & PAYRA S., 2022: Rapid flash flood calamity in Chamoli, Uttarakhand region during Feb 2021: an analysis based on satellite data. Natural Hazards, **112**, 1379-1393.

ZHOU, L., WANG, C., TANG, Y., ZHANG, B., ZHANG, H. & DONG, L., 2022: Interferometric SAR Observation of Permafrost Status in the Northern Qinghai-Tibet Plateau by ALOS, ALOS-2 and Sentinel-1 between 2007 and 2021. Remote Sensing, **14**(1870).